Evidence for Two Interconverting Protein Isomers in the Methotrexate Complex of Dihydrofolate Reductase from *Escherichia coli*†

Christopher J. Falzone,‡ Peter E. Wright,*,§ and Stephen J. Benkovic*,‡

Department of Chemistry, The Pennsylvania State University, 152 Davey Laboratory, University Park, Pennsylvania 16802, and Department of Molecular Biology, Research Institute of Scripps Clinic, 10666 North Torrey Pines Road, La Jolla, California 92037

Received September 28, 1990; Revised Manuscript Received November 14, 1990

ABSTRACT: Two-dimensional ^{1}H NMR methods and a knowledge of the X-ray crystal structure have been used to make resonance assignments for the amino acid side chains of dihydrofolate reductase from *Escherichia coli* complexed with methotrexate. The H7 proton on the pteridine ring of methotrexate was found to have NOEs to the methyl protons of Leu-28 which were assigned by using the L28F mutant. These NOEs indicated that the orientation of the methotrexate pteridine ring is similar in both solution and crystal structures. During the initial assignment process, it became evident that many of the resonances in this complex, unlike those of the folate complex, are severely broadened or doubled. The observation of two distinct sets of resonances in a ratio of approximately 2:1 was attributed to the presence of two protein isomers. At 303 K, NOESY spectra with mixing times of 100 ms did not show interconversion between these isomers. However, exchange cross-peaks were observed in a 700-ms NOESY spectrum at 323 K which demonstrated that these isomers are interconverting slowly on the NMR time scale. Many of the side chains with clearly doubled resonances were located in the β-sheet and the active site. Preliminary studies on the apoprotein also revealed doubled resonances in the absence of the inhibitor, indicating the existence of the protein isomers prior to methotrexate binding. In contrast to the methotrexate complex, the binary complex with folate and the ternary MTX–NADPH–DHFR complex presented a single enzyme form. These results are proposed to reflect the ability of folate and NADPH to bind predominantly to one protein isomer.

Dihydrofolate reductase (DHFR)[1] (5,6,7,8-tetrahydrofolate:NADP$^+$ oxidoreductase, EC 1.5.1.3) catalyzes the NADPH-dependent reduction of 7,8-dihydrofolate (H_2F) to 5,6,7,8-tetrahydrofolate. It is a monomeric protein consisting of 159 amino acids with a molecular mass of 18 000 daltons. DHFR is responsible for maintaining intracellular levels of tetrahydrofolate and its derivatives which are essential cofactors in the biosynthesis of purines, thymidylate, and several amino acids. Thus, DHFR is a target enzyme for a number of anti-folate drugs including the anticancer agent methotrexate (MTX) and the antibacterial compound trimethoprim. The inhibition of DHFR by these anti-folate drugs has been extensively studied [see Blakley (1984) for a review]. The stereochemistry of reduction (Charlton et al., 1979), recent crystallographic studies (Bystroff et al., 1990), and NMR spectroscopy results (Falzone et al., 1990) indicate that the conformation of bound MTX has the pteridine ring rotated about the C6–C9 bond by ca. 180° relative to that of dihydrofolate. In this orientation, hydrogen bonds are formed between the protein and the 2,4-diamino groups on the pyrimidine portion of the pteridine ring of MTX. In addition, a new hydrogen bond between a protonated N1 nitrogen of MTX and Asp-27 is also detected in the crystal structure (Bolin et al., 1982). Much of the enhanced affinity MTX has for DHFR over substrate has been attributed to this charge interaction (Blakley, 1984). The binding of MTX to DHFR is characteristic of a class of inhibitors that form an initial complex which isomerizes slowly to a tighter complex and are referred to as slow tight binding inhibitors (Morrison, 1982; Williams et al., 1979). Little is known about the nature of this slow isomerization or how MTX attains its final "upside-down" conformation. We wished to explore the interaction of MTX with DHFR in order to learn more about the final tight complex and the isomerization that led to its formation utilizing two-dimensional nuclear magnetic resonance methods.

Materials and Methods

Protein Purification and Sample Preparation. Wild-type DHFR and L28F DHFR (the latter provided by Dr. C. R. Wagner in our laboratory) were produced from cells (W71-18) that contained a plasmid possessing a subclone of the wild-type or mutant fol gene. W71-18 cells were grown in L-broth medium for ca. 12 h before being harvested by centrifugation. The proteins used in these experiments were purified and prepared as previously described (Falzone et al., 1990). Lyophilized proteins were dissolved in 0.35 mL of 99.96% ^2H_2O/200 mM KCl, and MTX was added in 1:1 to 1:3 molar ratios from a 50 mM stock solution [ϵ_{302} = 22 100 M^{-1} cm^{-1} in 0.1 M KOH (Stone et al., 1984)]. NADPH was added from a 110 mM stock solution (ϵ_{339} = 6200 M^{-1} cm^{-1}). Protein concentrations were determined spectrophotometrically by using a molar extinction coefficient of 31 100 M^{-1} cm^{-1} at 280 nm (Fierke et al., 1987). The pH of the protein solutions was 6.80 ± 0.03, and meter readings were not corrected for isotope effects. Final volumes were at least 0.4 mL and were 3–4 mM

†Supported by National Institutes of Health Grants GM 36643 to P.E.W. and GM 24129 to S.J.B. C.J.F. is supported by a fellowship from Merck, Sharp & Dohme.

‡The Pennsylvania State University.

§Research Institute of Scripps Clinic.

[1] Abbreviations: COSY, correlated spectroscopy; 1D, one dimensional; 2D, two dimensional; DHFR, dihydrofolate reductase; H_2F, 7,8-dihydrofolate; MTX, methotrexate; NOESY, two-dimensional proton nuclear Overhauser spectroscopy; 2Q, two-quantum spectroscopy; 2QF-COSY, double-quantum-filtered COSY; ROESY, rotating-frame Overhauser enhancement spectroscopy; TOCSY, total correlation spectroscopy.

0006-2960/91/0430-2184$02.50/0

in protein. For ^1H_2O samples, 90% ^1H_2O/10% ^2H_2O (200 mM KCl) was added after an initial lyophilization.

NMR Measurements. ^1H NMR spectra were recorded in ^2H_2O and 90% H_2O/10% ^2H_2O at 303 K with Bruker AM-500 and AM-600 spectrometers equipped with Aspect 3000 computers and digital-phase shifting hardware. Several spectra were collected at 323 K by using a Bruker AM-500 spectrometer. Quadrature detection in the ω_1 dimension was achieved by using time proportional phase incrementation (Bodenhausen et al., 1980; Marion & Wüthrich, 1983), and all spectra were processed and plotted in the phase-sensitive mode. The program FTNMR (written by Dr. Dennis Hare) was used to process all data on micro VAXII or CONVEX C240 computers. For all experiments, the carrier was placed on the solvent resonance, and 460–512 t_1 experiments consisting of 64, 96, or 128 transients were collected, each containing 2048 complex data points except for the NOESY, CAMELSPIN (ROESY), and TOCSY experiments, which contained 4096 complex points per experiment. The number of time domain points used in the transform and the relative strength of the sine-bell window function depended on whether high resolution or high sensitivity spectra were desired. Spectral widths in the F2 dimension for NOESY, TOCSY, and ROESY experiments were 12 500 Hz, and spectral widths in the F1 dimension for experiments other than 2Q were between 5800 and 6002 Hz (500 MHz) or 7002 Hz (600 MHz). The F1 spectral width for 2Q experiments was 10 000 Hz.

The pulse sequences and phase cycling routines for 2QF-COSY (Rance et al., 1983) and 2Q experiments (Braunschweiler et al., 1983; Rance & Wright, 1986) were standard. The spectral widths in the F2 dimension for correlation experiments were 7042 Hz at 600 MHz and 6024 Hz at 500 MHz. Mixing times for 2Q experiments were between 30 and 40 ms. Pure absorption Hahn-echo NOESY spectra (Bodenhausen et al., 1984; Davis, 1989) were collected with mixing times of 100 and 700 ms. TOCSY spectra were obtained according to the method of Rance (1987) using WALTZ-16 for spin-locking with a field strength of 6 kHz. The mixing times were 72 or 75 ms for TOCSY experiments. ROESY experiments were collected at 323 K by using the method of Bothner-By et al. (1984) with a spin-locking field of 2.5 kHz. For cosine-modulated data, the first free induction decay was divided by 2 to suppress t_1 ridges (Otting et al., 1986). All spectra were referenced to the $^1H^2HO$ line at 4.73 ppm for the experiments at 303 K and at 4.53 ppm for experiments at 323 K.

Results

Partial sequence-specific assignments for the ^1H NMR spectrum of the folate–DHFR complex have been made previously by using site-directed mutagenesis, a knowledge of the wild-type DHFR–MTX X-ray crystal structure (Bolin et al., 1982), and observation of unique networks of intraresidue NOE connectivities consistent with the solid-state predictions (Falzone et al., 1990). Assignments for the MTX complex have been made by applying similar methods. Of special interest to this report is the assignment of Leu-28. The methyl groups and the C^γ proton of this side chain were assigned unambiguously through the L28F mutant as in the folate complex (Falzone et al., 1990). For many residues, chemical shift differences between identical protons in the folate and MTX complexes were less than 0.05 ppm. For several others, particularly those in the active site, proton resonances were shifted by more than 0.1 ppm or were severely broadened in the MTX–DHFR complex. In some cases, side-chain spin systems that could be completely identified in spectra of the folate complex could only be partially identified in those of the MTX complexes; thus, assignments are somewhat less complete in the latter than in the former. Table I summarizes the assignments for the DHFR–MTX complex.

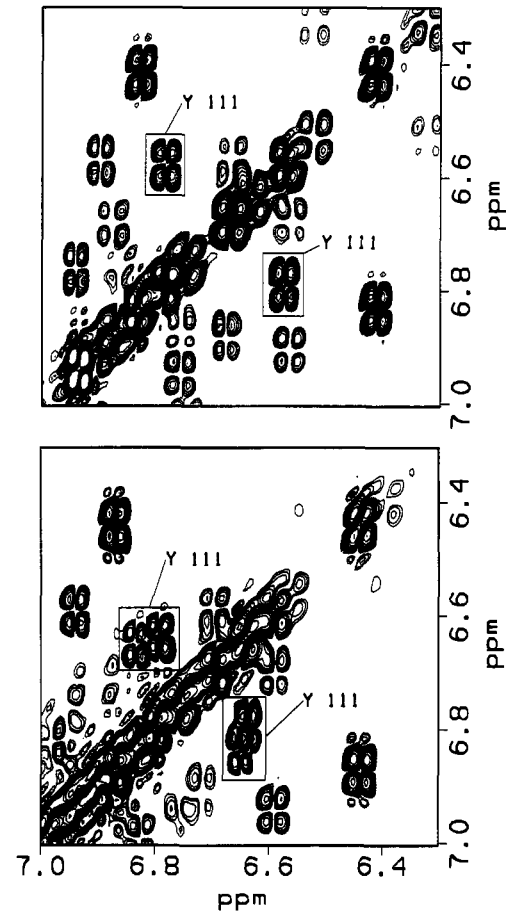

FIGURE 1: Region of 2QF-COSY spectrum showing Tyr-111 $C^\delta H$ and $C^\epsilon H$ cross-peaks in the binary folate–DHFR complex (top) and the corresponding region of the MTX–DHFR complex (bottom). Note the selective doubling of these cross-peaks in the MTX complex.

From the initial comparison of the NMR spectra of the folate and MTX complexes of DHFR, it is clear that important structural differences exist. The most obvious difference for the MTX binary complex is that there is doubling of side-chain proton resonances for some, but not all, residues. Figure 1 (top) contains a section of the aromatic region in the 2QF-COSY spectrum of the binary folate complex showing the $C^\delta H/C^\epsilon H$ cross-peaks for Tyr-111; Figure 1 (bottom) presents the same region of the spectrum in the MTX complex and shows clearly two cross-peaks corresponding to Tyr-111. Many aliphatic protons are also affected by this isomerization as illustrated in Figure 2. For example, Figure 2A shows the $C^\gamma H–C^\delta H_3$ cross-peaks of Leu-112 in the folate complex; this set of cross-peaks is doubled in the MTX complex (Figure 2B). Figure 2C shows the $C^\beta H–C^\gamma H_3$ 2QF-COSY cross-peaks for Val-93 and the Ile-94 $C^\beta H–C^\gamma H_3$ cross-peak in the DHFR–folate complex; in the DHFR–MTX complex, these cross-peaks are also doubled (Figure 2D). Interresidue NOEs can be observed from each unique chemical shift of amino acid side chains that possess two sets of resonances. For example, the $C^\delta H_2$ protons of Tyr-111 are doubled, with chemical shifts of 6.79 and 6.84 ppm (Figure 1). The $C^\delta H_2$ protons at 6.79 ppm give rise to an NOE to one of the doubled $C^\gamma H_3$ resonances of Ile-155 at 0.47 ppm while the $C^\delta H_2$ protons at 6.84 ppm show an NOE to the other $C^\gamma H_3$ at 0.48 ppm (data not shown). These interresidue NOEs can be used to assign

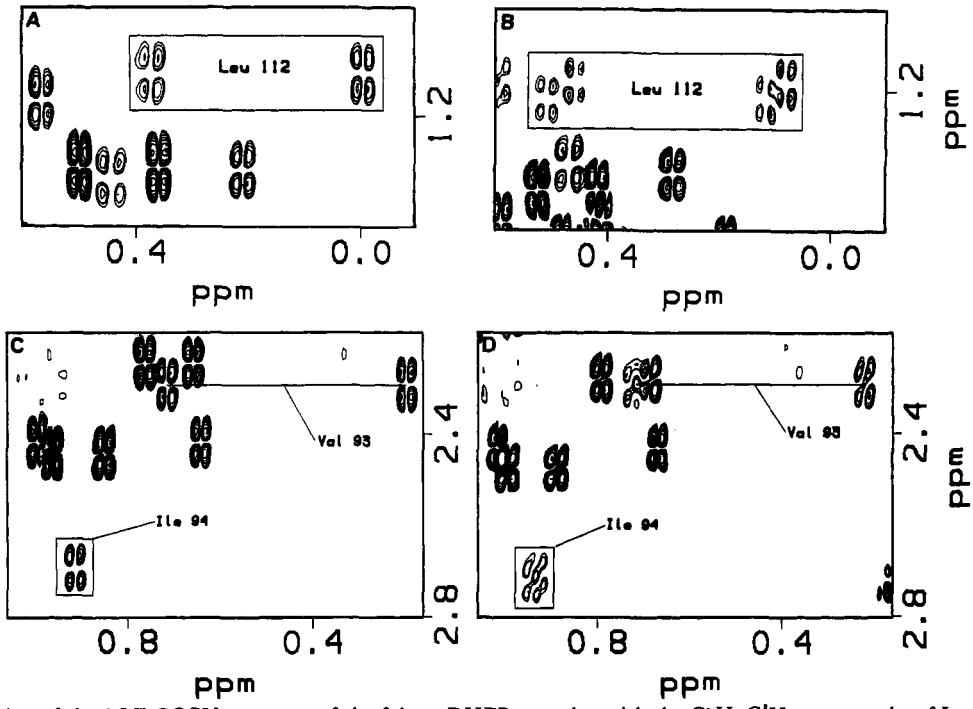

FIGURE 2: (A) Region of the 2QF-COSY spectrum of the folate–DHFR complex with the $C^{\gamma}H$–$C^{\delta}H_3$ cross-peaks of Leu-112 indicated and (B) the corresponding region for the MTX–DHFR complex which shows resonances for this residue in two distinct environments. (C) Region of the 2QF-COSY of the folate–DHFR complex with both $C^{\beta}H$–$C^{\gamma}H_3$ cross-peaks of Val-93 and the $C^{\beta}H$–$C^{\gamma}H_3$ cross-peak of Ile-94 indicated. (D) The corresponding region of the MTX–DHFR complex showing the doubling of these cross-peaks.

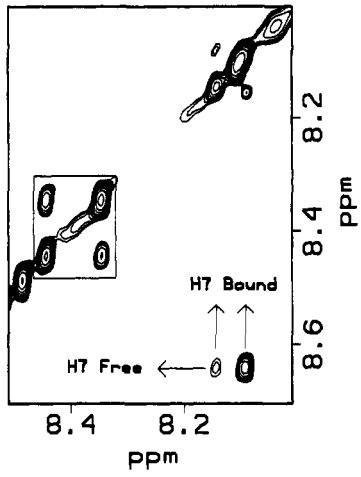

FIGURE 3: Region of a 700-ms NOESY spectrum at 323 K. Under these conditions, the $C^{\epsilon}H$ of His-124 (box) shows a saturation-transfer cross-peak indicative of interconversion between the two protein forms during the mixing time. The arrows indicate the two exchange cross-peaks for the MTX H7 resonance in the free and bound states.

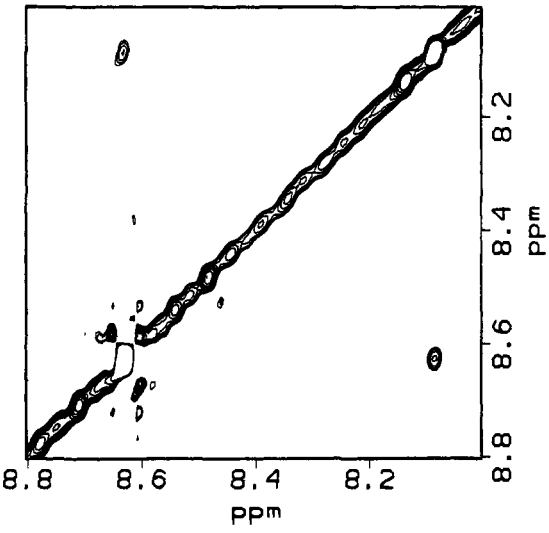

FIGURE 4: Region of a 200-ms ROESY spectrum at 323 K showing the exchange cross-peak for H7 of MTX. Only positive levels (exchange cross-peaks and diagonal) are plotted. An exchange cross-peak is seen to only one of the bound species; the other is too weak to detect.

specific residues within each form. Table II lists the assigned residues that give rise to two sets of resonances and their location in the protein.

The presence of two sets of distinct resonances suggests the occurrence of two protein isomers that interconvert slowly on the NMR time scale. No exchange cross-peaks between well-resolved doubled resonances could be found in the 100-ms NOESY spectrum at 303 K, indicating that if the two protein species interconvert, the process is not fast enough to be detected within this mixing time. However, by elevation of the temperature to 323 K and lengthening of the NOESY mixing time to 700 ms, interconversion between the two enzyme isomers can be detected through the appearance of exchange cross-peaks between some of the doubled resonances, e.g., between the $C^{\epsilon}H$ resonance of His-124 in its two environments as seen in Figure 3. Exchange cross-peaks, when they can be resolved from the diagonal, are also detected for other doubled resonances. Furthermore, under these conditions and with a 3-fold excess of MTX, the free H7 resonance is readily recognized at 8.64 ppm. Saturation transfer is observed among the free and *two* bound forms of the inhibitor (Figure 3). A ROESY experiment was performed to distinguish between exchange and NOE cross-peaks: exchange cross-peaks and the diagonal are negative whereas NOE cross-peaks are positive. The 200-ms ROESY spectrum presented in Figure 4 shows the exchange between H7 of free MTX and one of the bound forms, the other is apparently too weak to detect in this experiment.

To investigate the possibility that two protein isomers exist in solution prior to binding substrate or inhibitor, 2QF-COSY and 100-ms NOESY spectra were collected with apo-DHFR.

Table I: Chemical Shifts (±0.01 ppm) of Assigned Residues in the DHFR–MTX Complex from *E. coli* (pH 6.8, T = 303 K)

	$C^{\delta}H$	$C^{\epsilon}H$	$C^{\zeta}H$
Phe-31	6.93	7.30	7.05
Phe-31	6.92	7.27	7.01
Phe-103	7.59	7.14	7.14
Phe-125	7.12	6.23	6.64
Phe-137	7.30	7.44	7.58
Phe-137	7.32	7.47	7.60
Phe-153	6.82	6.98[a]	
Phe-153	6.76	6.96[a]	
Tyr-100	7.06	7.18	
Tyr-111	6.79	6.64	
Tyr-111	6.84	6.65	
Tyr-128	6.87	6.44	

	$C^{\delta}H$	$N^{\epsilon}H$	$C^{\beta 2}H$	$C^{\eta}H$	$C^{\beta 3}H$	$C^{\epsilon 3}H$
Trp-22	6.94	10.29	7.22	6.92	6.72[b]	
Trp-47	7.26	10.23	7.44	6.56	6.40	7.50
Trp-74	7.24	10.05	7.02	6.76	6.99	7.57
Trp-133	7.97	10.34[c]	7.35	6.69	6.59	6.94

	$C^{\epsilon}H$	$C^{\delta}H$		$C^{\epsilon}H$	$C^{\delta}H$
His-45	8.27	7.30	His-124	8.60	7.41
His-45	8.28	7.35	His-141	8.55	6.23
His-114	7.72	6.70	His-141	8.59	6.34
His-114	7.80	6.75	His-149	7.85	7.23
His-124	8.49	7.40			

	$C^{\alpha}H$	$C^{\beta}H_3$		$C^{\alpha}H$	$C^{\beta}H_3$
Ala-6	4.88	0.87	Ala-9	5.40	1.57
Ala-6	4.90	0.84	Ala-81	4.01	1.72
Ala-7	4.90	1.23	Ala-107	4.66	1.81
Ala-9	5.13	1.68			

	$C^{\gamma}H$	$C^{\delta}H_3$	$C^{\delta}H_3$
Leu-8	1.38	0.42	0.53
Leu-8	1.44	0.41	0.59
Leu-28	1.57	0.15	0.55
Leu-28	1.47	0.19	0.48
Leu-54	1.75	0.62	0.93
Leu-54	1.74	0.61	0.93
Leu-62	1.48	0.64	0.83
Leu-110	0.79	−0.75	0.61
Leu-110	0.75	−0.75	0.59
Leu-112	1.19	0.09	0.46
Leu-112	1.21	0.12	0.51
Leu-156	1.60	0.70	0.91
Leu-156	1.58	0.68	0.91

	$C^{\beta}H$	$C^{\gamma}H_3$	$C^{\gamma}H_3$
Val-10	2.12	1.07	1.10
Val-10	2.15	1.07	1.13
Val-72	1.35	−0.45	0.29
Val-75	2.28	0.69	0.79
Val-78	1.87	0.47	0.56
Val-93	2.28	0.22	0.72
Val-93	2.30	0.22	0.71

	$C^{\beta}H$	$C^{\gamma}H_2$	$C^{\gamma}H_3$	$C^{\delta}H_3$
Ile-5	1.31	1.75, 2.24	1.06	0.37
Ile-5	1.31	1.81, 2.24	1.06	0.38
Ile-41	1.18	0.58, 1.34	0.59	0.47
Ile-41	1.19	0.60, 1.34	0.61	0.47
Ile-61	0.86	−0.26, 0.05	0.30	−0.50
Ile-82	1.97	1.14, 2.14	0.96	0.99
Ile-94	2.70		0.93[d]	
Ile-94	2.72		0.94	
Ile-115	0.99	0.06, 1.05	0.29	−0.60
Ile-155	1.70	0.97, 1.95	0.47	0.68
Ile-155	1.72	0.99, 1.95	0.48	0.69

	$C^{\beta}H$	$C^{\gamma}H_3$
Thr-35	3.48	0.18
Thr-73	3.84	1.15
Thr-113	3.99	0.85

MTX	H-7	$N10-CH_3$
	8.13	3.34
	8.18	3.18

[a] The $C^{\zeta}H$ has not been assigned in either form. [b] The $C^{\epsilon 3}H$ has not been assigned. [c] The $C^{\delta}H$ and the $N^{\epsilon}H$ have a second set of resonances at 7.95 and 10.30 ppm, respectively. [d] The $C^{\delta}H_3$ and $C^{\gamma}H_2$ protons remain unassigned.

Table II: Residues That Show Distinct Resonances in Both Protein Isomers As Observed in 2QF-COSY and Their Location in the Secondary Structure of the *E. coli* DHFR–MTX X-ray Crystal Structure (Bolin et al., 1982)

residue	location	residue	location
Ile-5	βA strand	Ile-94	βE strand, active site
Ala-6	βA strand	Leu-110	βF strand
Leu-8	βA strand	Tyr-111	βF strand
Ala-9	loop after βA strand	Leu-112	βF strand
Val-10	loop after βA strand	His-114	βF strand
Leu-28	αB helix, active site	His-124	surface
Phe-31	αB helix, active site	Phe-137	βG strand
Ile-41	βB strand	His-141	βG strand
His-45	αC helix	Phe-153	βH strand
Leu-54	active site	Ile-155	βH strand
Val-93	βE strand	Leu-156	βH strand

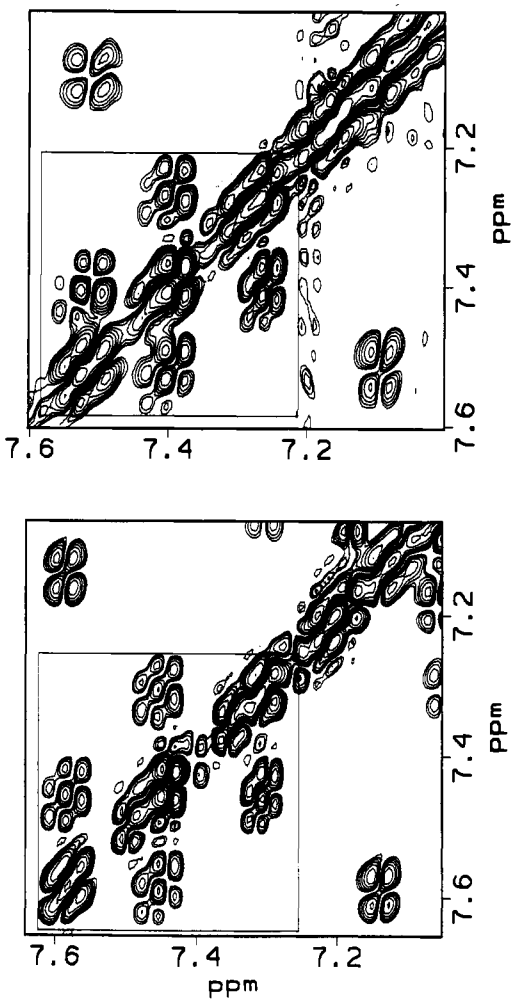

FIGURE 5: 2QF-COSY spectra of the MTX–DHFR complex (bottom) and apo-DHFR (top). Inside of each box are the doubled cross-peaks of Phe-137.

Although the quality of the spectra was not as good as that of the binary complexes with folate or MTX, many residues, particularly outside of the active site, can be assigned by using the same methods as described above. The salient feature of the apoprotein spectra is that some residues give rise to two sets of resonances as in the spectra of the MTX complex. These residues include His-45, Val-93, Leu-110, Tyr-111, Leu-112, His-124, Phe-137, and Leu-156. Figure 5 shows the cross-peaks for Phe-137 exhibiting a similar pattern of doubling in both the MTX complex (bottom) and apo-DHFR (top). It should be noted that all the residues that are doubled in the MTX complex were also doubled in the apoprotein when they could be assigned.

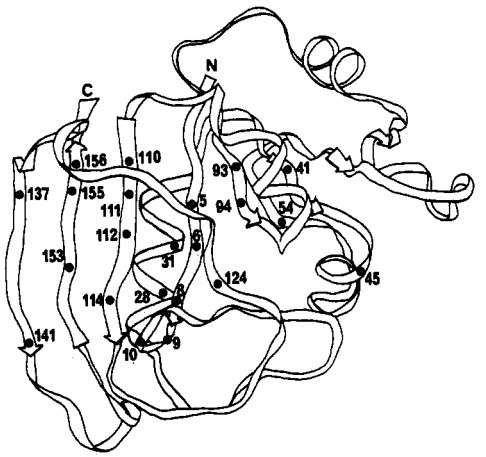

FIGURE 6: Ribbon diagram of *E. coli* DHFR based on the X-ray crystal structure of the MTX complex (Bolin et al., 1982), indicating the assigned residues whose side-chain proton resonances are doubled.

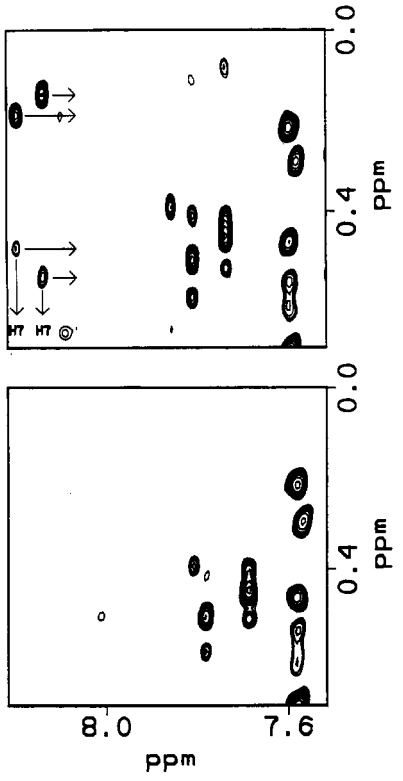

FIGURE 7: Region of the wild-type DHFR–MTX 100-ms NOESY spectrum at 303 K (top) showing NOEs between the two bound H7 resonances and the doubled resonances of Leu-28. These NOEs disappear in the 100-ms NOESY spectrum of the L28F DHFR–MTX (bottom).

Assigned residues which show two sets of resonances in the MTX complex are located predominantly in the eight-stranded β-sheet of DHFR and in the active site. These residues are indicated in a ribbon representation (Figure 6) of the DHFR–MTX X-ray crystal structure (Bolin et al., 1982). The active-site residues which produce distinct resonances in each form include Ile-5, Leu-28, Phe-31, Leu-54, and Ile-94. The extent of this isomerization, though significant, is not global, and several residues within 4 Å of those listed in Table II do not seem to be directly involved in this isomerization at least as manifested in chemical shift perturbation.

Figure 7 (top) shows the NOE cross-peaks of the two bound H7 resonances of MTX at 8.13 and 8.18 ppm in the 0.6–0.0 ppm region of the spectrum. Each bound H7 is in contact with the methyl groups of a Leu or Val side chain with chemical

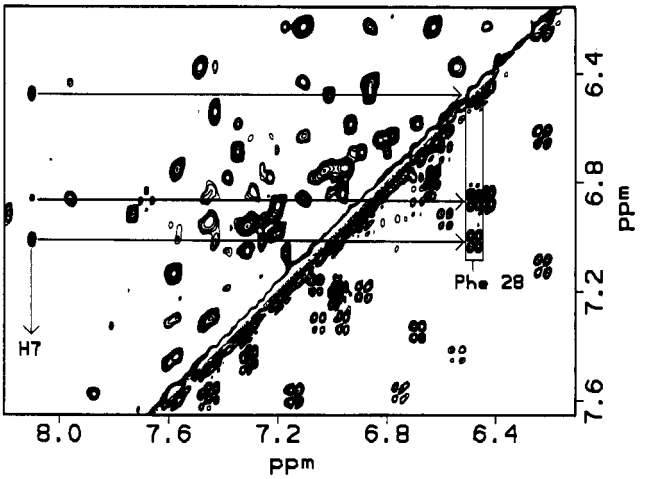

FIGURE 8: Region of a 100-ms NOESY spectrum (above the diagonal) of the L28F DHFR–MTX showing NOEs between one bound H7 resonance and the ring protons of Phe-28 shown below the diagonal in a 2QF-COSY spectrum. Both spectra were collected at 303 K.

shifts similar to those of Leu-28 in the folate–DHFR complex. Given the presence of two protein isomers, one or *both* of these isopropyls can be considered as candidates for Leu-28 in the MTX complex. The only methyls within 8 Å of H7 in the crystal structure belong to Leu-28 (2.7 Å, closest methyl proton) and Leu-24 (7.8 Å, closest methyl proton). Therefore, Leu-28 is most likely the residue showing NOEs to MTX H7. To confirm this assignment, and to investigate the effects that a mutation in the active site might have on this isomerization, the L28F DHFR–MTX complex was examined and compared to the wild-type DHFR–MTX complex.

The L28F DHFR–MTX spectra are similar to wild-type spectra and show a nearly identical pattern of doubled resonances. Figure 8 shows the appearance of a new phenyl spin system in the 2QF-COSY spectrum of L28F DHFR which can be assigned as Phe-28. Unlike Leu-28, the two forms of Phe-28 are not well resolved. In addition, there is a sharp resonance at 8.10 ppm which we assign to one of the bound MTX H7 protons with NOEs to all protons of this Phe ring spin system (Figure 8, above the diagonal). Assignment of the second bound MTX H7 is best accomplished by observing saturation-transfer cross-peaks in a 700-ms NOESY spectrum at 323 K as described above for the wild-type protein. As illustrated in Figure 9, it is found at 8.13 ppm at 323 K. This second bound H7 resonance exhibits NOEs to the second form of Phe-28 (overlapping with the first at this temperature). This indicates a similar orientation for the pteridine ring. Interestingly, the NOEs between the bound H7 protons of MTX and the ring protons of Phe-28 show different intensities in the two isomers which reflect conformational differences between the bound forms. These differences are currently under investigation. Figure 7 (bottom) shows the disappearance of NOEs from H7(s) to leucine methyls in the L28F protein that were observed in the wild-type NOESY spectrum. There is a concomitant loss of the methyl resonances at ~0.2 ppm in the 2QF-COSY spectrum of L28F DHFR. The two resonances at about 0.6 ppm are also removed by the mutation although being in a relatively crowded region, their disappearance is less obvious. Both sets of methyls with NOEs to the two bound H7 protons are assigned to Leu-28.

The NOEs observed between the residue at position 28 and bound MTX H7 are important because they prove the orientation of the pteridine ring is similar in the two forms for both wild-type and L28F proteins. In addition, intrainhibitor NOEs between both bound H7 and the N10–CH_3 resonances

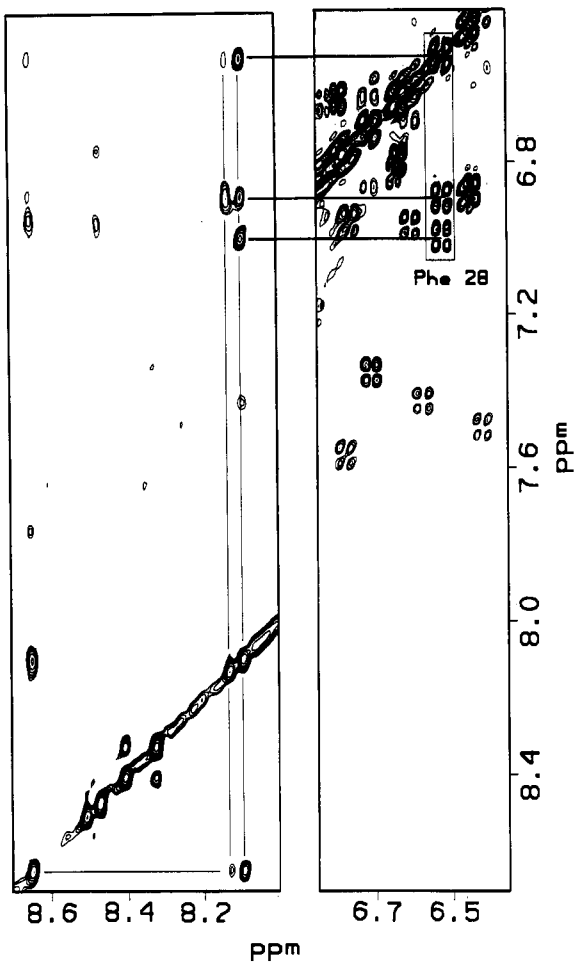

FIGURE 9: Regions of a 700-ms NOESY spectrum (left) and 2QF-COSY spectrum (right) at 323 K for the L28F DHFR–MTX complex. In this experiment, two bound H7 resonances can be assigned, both with NOEs to Phe-28.

are also detected. All of these NOEs, which are not expected for a folate conformation, are indicative of a nonproductive pteridine ring orientation. Therefore, the orientation of the pteridine ring in solution resembles the X-ray crystal structure (Bolin et al., 1982).

To investigate whether forming the ternary complex with NADPH perturbs the relative population of the two enzyme–MTX forms, the NADPH–MTX–DHFR complex was examined. Figure 10A shows the two sets of 2QF-COSY $C^{\gamma}H$–$C^{\delta}H_3$ cross-peaks for the Leu-28 side chain found in the binary MTX–DHFR complex. As noted above, these methyls have NOEs to the two bound H7 protons on the pteridine ring of MTX (Figure 7, top). However, in the ternary complex (Figure 10B), only *one* set of methyls for Leu-28 is found with NOEs to *one* bound H7 on MTX. Figure 10B also shows the Ile-155 $C^{\beta}H$–$C^{\gamma}H_3$ cross-peak which is not doubled in the ternary complex as it was in the binary complex (Figure 10A). In fact, all other doubled resonances are now found in a single environment in the ternary complex, indicating that the binding of NADPH has driven the observed equilibrium into one enzyme form.

Discussion

The binary MTX–DHFR complex reveals two bound enzyme forms which cannot be detected in the binary complex with folate. Interconversion between these two forms, which is slow on the NMR time scale, can be shown to occur by observation of exchange cross-peaks in a 700-ms NOESY spectrum at 323 K. Overall, the data are consistent with

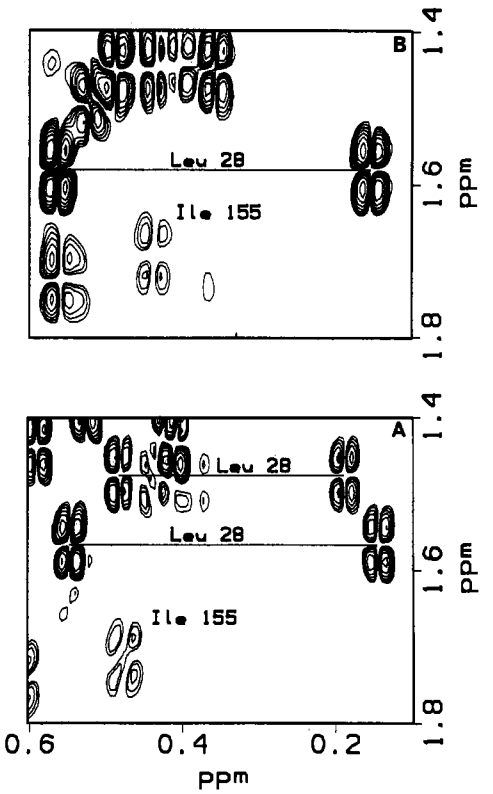

FIGURE 10: (A) Region of a 2QF-COSY spectrum showing the two sets of $C^{\gamma}H$–$C^{\delta}H_3$ cross-peaks of Leu-28 and the $C^{\beta}H$–$C^{\gamma}H_3$ cross-peaks of Ile-155 in the MTX–DHFR complex. (B) Ternary MTX–NADPH–DHFR complex with these same cross-peaks now showing a single set of cross-peaks. A single H7 resonance is detected with NOEs to the methyls of Leu-28 (data not shown). Note that some resonances have shifted in the ternary complex but residues with two distinct sets of cross-peaks in the binary complex (Table II) now only have one set.

Scheme I

$$\begin{array}{ccccc} E_A & + & MTX & \rightleftharpoons & E_A \cdot MTX \\ \Updownarrow & & & & \Updownarrow \\ E_B & + & MTX & \rightleftharpoons & E_B \cdot MTX \end{array}$$

Scheme I where the isomerization steps involve changes in the protein conformation only. Integration of resolved doubled resonances (e.g., those of His-124 $C^{\epsilon}H$ and H7) in the 1D spectra demonstrates that MTX has only a slight (ca. 2:1) preference for binding to one of the two forms of *E. coli* DHFR.

The model of Scheme I provides the most economical representation of the data and is supported by several observations: (a) Intrainhibitor NOEs as well as protein–inhibitor NOEs indicate the conservation of geometric relationships in the two bound forms. Minor differences would not be expected to cause the extensive perturbation detected through the β-sheet and involving residues distal to bound MTX. (b) The observation that MTX can bind to two *E. coli* apoenzyme forms was first reported by Cayley et al. (1981) on the basis of stopped-flow fluorescence quenching studies. It is consistent with the specific doubling of resonances detected in our NMR experiments. In contrast, H_2F and NADPH seem to bind to only one form in *E. coli* DHFR (Cayley et al., 1981; Fierke et al., 1987). The absence of doubled protein resonances in the binary folate–enzyme complex (Falzone et al., 1990) or the MTX–NADPH–enyzme complex is also consistent with earlier kinetic results. (c) The apoprotein shows the doubling of specific residues. These residues, when they can be assigned, are also doubled in the MTX complex. The existence of two

stable conformations for *Streptococcus faecium* DHFR has also been reported (London et al., 1979). In this study, two of the four $^{13}C^{\gamma}$-labeled tryptophans showed doubled ^{13}C resonances which is consistent with our apo-DHFR data.

The extensive isomerization involves at least six of the eight strands of the β-sheet and residues in the active site. The largest perturbations, in terms of chemical shift, seem to be centered in the domain containing the long strands of the β-sheet (A, F, H, and G strands) with the effects of the isomerization being tapered toward the four shorter stands (E, B, C, and D) of the β-sheet. For example, residues in the αE helix, which is docked on the short β-strands, show no discernible chemical shift perturbations stemming from the isomerization. This isomerization also affects the active-site residues including those of the αB helix (Leu-28 and Phe-31). The active-site residues Ile-5, Leu-54, and Ile-94 are also perturbed. Other residues may also participate in this isomerization such as Trp-22, but their partner set of resonances cannot be assigned unambiguously at this time. The precise structural differences between the two forms as well as quantitating the rate of interconversion is under investigation. Evidence for this isomerization was not clearly found in the binary MTX solid-state structure (Bolin et al., 1982). Recent X-ray data on human DHFR with folate did find minor structural differences between the two enzyme molecules in the unit cell (Davies et al., 1990). The relationship to the *E. coli* enzyme forms observed in this study is unknown.

The role that this isomerization plays in the slow onset of tight MTX inhibition is open to conjecture. In *E. coli* DHFR, the E_A·MTX $\rightarrow$ E_B·MTX isomerization does little to tighten the binding. The stopped-flow progress of inhibition experiments of Appleman et al. (1988) revealed a slow isomerization of E·NADPH·MTX which decreased the K_D only by a factor of 2.4. This is consistent with our binary complex results. If the isomerization reported here is responsible for forming the final tight complex, then it is possible that DHFRs which exhibit a greater K_D ratio than *E. coli* DHFR would show a single set of E·MTX resonances in the NMR spectrum.

King and co-workers (Dunn et al., 1978; Dunn & King, 1980; Cayley et al., 1981) have characterized two forms of apo-DHFR (referred to as E_1 and E_2) using stopped-flow fluorescence kinetics. The equilibrium mixture of these two forms consists of about 50% E_1 (active conformer) and 50% E_2 in *E. coli* DHFR (Adams et al., 1989; Fierke et al., 1987); the interconversion between E_1 and E_2 is slow (0.035 s^{-1}) (Chen et al., 1987). It has also been reported that for *E. coli* DHFR, MTX readily binds both forms of the enzyme (Cayley et al., 1981) whereas folate and NADPH show little affinity for the E_2 form (Adams et al., 1989; Appleman et al., 1990). These kinetic results are in concert with our NMR data. The detection of two forms of apo-DHFR which share characteristics of the two bound MTX forms suggests that our E_A and E_B may correspond, or at least be related, to Cayley's kinetically distinguishable E_1 and E_2 forms. If E_1 and E_2 were not responsible for the specific doubling of residues observed in the binary MTX complex, then two slow processes would have to exist. The inability to observe exchange cross-peaks at 303 K in 100-ms NOESY experiments is consistent with slowly interconverting enzyme species.

The structural differences between the two observed enzyme forms, which involve active-site residues intimately associated with binding the pterin ring of H_2F, must incorporate the ability of one form to bind the substrate and cofactor readily and the other to present little affinity for it. DHFRs from other species exhibit the E_1/E_2 equilibrium (Dunn et al., 1978; Thillet et al., 1990) which indicates that common interspecies structural features are responsible for its existence. Some site-directed mutants have been shown to perturb the equilibrium between the E_1 and E_2 forms (Chen et al., 1987; Appleman et al., 1990) although the cause of this perturbation is unknown. The physiological significance of these two enzyme forms is also unknown.

NOEs between the bound H7 resonances of MTX and Leu-28 in wild-type DHFR indicate that the orientation of the pteridine ring is similar for both protein isomers: this is the orientation of the pteridine ring in the X-ray crystal structure. If the pteridine ring of MTX is to sample an active conformation (i.e., rotated 180° about the C6–C9 bond when compared to the crystal structure), it must do so transiently upon initial encounter before attaining its observed crystal structure-like orientation. This can be contrasted to the folate complex where NOEs from bound H7 to Leu-28 are not observed but NOEs to $C^{\gamma}H_3$ of Ile-5 and $C^{\beta}H$ of Ile-94 are seen (Falzone et al., 1990). These latter NOEs clearly indicate that the pterin ring is oriented in the active form, poised for reduction (Charlton et al., 1979). Also in the folate complex, only one bound H7 resonance is found at pH 6.8 and 303 K. Moreover, the inability of H_2F to bind to both protein isomers in *E. coli* DHFR (Fierke et al., 1987) is consistent with the lack of doubled resonances observed in these complexes. These data for the folate complex are also consistent with kinetic data (Fierke et al., 1987) which show a burst amplitude equal to the active protein concentration, indicating that substrate is not involved in kinetically significant nonproductive conformations prior to turnover.

The replacement of the carbonyl oxygen by an amino group at the 4-position in the pteridine ring produces profound effects: it favors an all-MTX-like orientation of the pteridine ring for *E. coli* DHFR and allows binding to two forms of the enzyme. Evidently, some structural element of *E. coli* DHFR in an E_2-like form does not allow substrate (carbonyl at the 4-position) to bind at detectable levels. To contrast these differences between substrate and inhibitor binding, some details of the folate and MTX complexes with *Lactobacillus casei* DHFR should be noted. In binary complexes, folate produces doubled resonances in *L. casei* DHFR, and its pterin ring has been shown to exist in two distinct environments whereas in the MTX complex, the doubling of resonances is not detected and its pteridine ring seems to bind in one conformation (Birdsall et al., 1989). The multiple modes of binding in the folate complex observed with *L. casei* DHFR place the pterin ring in an active conformation and in an MTX-like conformation (Birdsall et al., 1989). If the origins of the multiple binding modes are similar for the two species of DHFR, it is possible that the MTX-like conformation of folate bound to *L. casei* DHFR arises from binding to the inactive enzyme form. *E. coli* DHFR shows no propensity for folate to bind this inactive form despite its relatively high active-site homology (55% H_2F site) with the *L. casei* protein (Benkovic et al., 1988). A subtle change in the protein structure from *E. coli* to *L. casei* may have changed the binding specificity of the protein isomers for MTX and folate. It is possible that some other source of DHFR or an engineered version could bind both substrate and inhibitor in its two forms detectable by NMR methods.

Elucidating the structural elements responsible for the differential binding of inhibitor and substrate by the two enzyme isomers using site-directed mutagenesis would enhance our ability to create enzymes with desired kinetic properties. Characterization of the structural features of the two enzyme

forms is in progress, and it is expected that the design of more selective inhibitors will benefit from a knowledge of subtle interspecies structural differences exhibited by various DHFRs.

ACKNOWLEDGMENTS

Stimulating discussions with Drs. J. T. J. Lecomte and C. R. Matthews are gratefully acknowledged.

REFERENCES

Adams, J., Johnson, K., Matthews, R., & Benkovic, S. J. (1989) *Biochemistry 28*, 6611–6618.

Appleman, J. R., Howell, E. E., Kraut, J., Kühl, M., & Blakley, R. L. (1988) *J. Biol. Chem. 263*, 9187–9198.

Appleman, J. R., Howell, E. E., Kraut, J., & Blakley, R. L. (1990) *J. Biol. Chem. 265*, 5579–5584.

Benkovic, S. J., Fierke, C. A., & Naylor, A. M. (1988) *Science (Washington, D.C.) 239*, 1105–1110.

Birdsall, B., Feeney, J., Tendler, S. J. B., Hammond, S. J., & Roberts, G. C. K. (1989) *Biochemistry 28*, 2297–2305.

Blakley, R. L. (1984) in *Folates and Pterins. Chemistry and Biochemistry of Folates* (Blakley, R. L., & Benkovic, S. J., Eds.) Vol. 1, pp 191–253, Wiley, New York.

Bodenhausen, G., Vold, R. L., & Vold, R. R. (1980) *J. Magn. Reson. 37*, 93–106.

Bodenhausen, G., Kogler, H., & Ernst, R. R. (1984) *J. Magn. Reson. 58*, 370–388.

Bolin, J. T., Filman, D. J., Matthews, D. A., Hamlin, R. C., & Kraut, J. (1982) *J. Biol. Chem. 257*, 13650–13662.

Bothner-By, A. A., Stephens, R. L., Lee, J., Warren, C. D., & Jeanloz, R. W. (1984) *J. Am. Chem. Soc. 106*, 811–813.

Braunschweiler, L., Bodenhausen, G., & Ernst, R. R. (1983) *Mol. Phys. 48*, 535–560.

Bystroff, C., Oatley, S. J., & Kraut, J. (1990) *Biochemistry 29*, 3263–3277.

Cayley, P. J., Dunn, S. M. J., & King, R. W. (1981) *Biochemistry 20*, 874–879.

Charlton, P. A., Young, D. W., Birdsall, B., Feeney, J., & Roberts, G. C. K. (1979) *J. Chem. Soc., Chem. Commun.*, 922–924.

Chen, J.-T., Taira, K., Tu, C.-P. D., & Benkovic, S. J. (1987) *Biochemistry 26*, 4093–4100.

Davies, J. F., Delcamp, T. J., Prendergast, N. J., Ashford, V. A., Freisheim, J. H., & Kraut, J. (1990) *Biochemistry 29*, 9467–9479.

Davis, D. G. (1989) *J. Magn. Reson. 81*, 603–607.

Dunn, S. M. J., & King, R. W. (1980) *Biochemistry 19*, 766–773.

Dunn, S. M. J., Batchelor, J. G., & King, R. W. (1978) *Biochemistry 17*, 2356–2364.

Falzone, C. J., Benkovic, S. J., & Wright, P. E. (1990) *Biochemistry 29*, 9667–9677.

Fierke, C. A., Johnson, K. A., & Benkovic, S. J. (1987) *Biochemistry 26*, 4085–4092.

London, R. E., Groff, J. P., & Blakley, R. L. (1979) *Biochem. Biophys. Res. Commun. 86*, 779–786.

Marion, D., & Wüthrich, K. (1983) *Biochem. Biophys. Res. Commun. 113*, 967–974.

Morrison, J. F. (1982) *Trends Biochem. Sci. 7*, 102–105.

Otting, G., Widmer, H., Wagner, G., & Wüthrich, K. (1986) *J. Magn. Reson. 66*, 187–193.

Rance, M. (1987) *J. Magn. Reson. 74*, 557–564.

Rance, M., & Wright, P. E. (1986) *J. Magn. Reson. 66*, 372–378.

Rance, M., Sørensen, O. W., Bodenhausen, G., Wagner, G., Ernst, R. R., & Wüthrich, K. (1983) *Biochem. Biophys. Res. Commun. 117*, 479–485.

Stone, S. R., Montgomery, J. A., & Morrison, J. F. (1984) *Biochem. Pharmacol. 33*, 175–179.

Thillet, J., Adams, J. A., & Benkovic, S. J. (1990) *Biochemistry 29*, 5195–5202.

Williams, J. W., Morrison, J. F., & Duggleby, R. G. (1979) *Biochemistry 18*, 2567–2573.